UTILIZING DIGITAL LIGHT PROCESSING AND COMPRESSED SENSING FOR PHOTOCURRENT MAPPING OF ENCAPSULATED PHOTOVOLTAIC MODULES

George Koutsourakis[a], Martin Bliss[b], Thomas R Betts[b] and Ralph Gottschalg[c,d]
[a] National Physical Laboratory (NPL), Hampton Road, Teddington, Middlesex, TW11 0LW, UK
[b]Centre for Renewable Energy Systems Technology (CREST), Wolfson School Mechanical, Electronic and Manufacturing Engineering, Loughborough University, Loughborough, Leicestershire, LE11 3TU, UK
[c] Fraunhofer-Center for Silicon-Photovoltaic (CSP), Otto-Eissfeldt-Straße 12, 06120 Halle
[d] Fachbereich Elektrotechnik, Maschinenbau und Wirtschaftsingenieurwesen (EMW), Hochschule Anhalt, Bernburger Str.57 06366 Köthen

ABSTRACT: Photocurrent mapping can provide useful spatial information about the electrical and optical properties of a photovoltaic (PV) device under actual operating conditions. Although it is a well-established technique for PV cells, direct current mapping measurements of PV modules is impractical and time-consuming to be applied. One has to mechanically shade specific cells of the PV module or destructively access the cell to be measured. In this work, non-destructive, automated current mapping of encapsulated PV modules is demonstrated. A commercial Digital Light Processing (DLP) projector is utilised in order to apply compressive sampling for current mapping of PV modules. This method is non-destructive, cost effective and significantly fewer measurements are needed for acquiring a current map compared to raster scanning methods. When applying compressive sampling, a series of patterns is projected on the sample, the current response is measured for each pattern and the current map is acquired using an optimisation algorithm. Specific shading strategies, voltage bias settings and I-V curve details are investigated for optimised compressive sampling.

Keywords: Current mapping, Compressed sensing, Non-destructive testing, PV modules

1 INTRODUCTION

Accessing the electrical parameters of individual cells in encapsulated photovoltaic (PV) modules is not an easy task. Several methodologies have been demonstrated in order to achieve this, most based on mechanical shading of cells. Dark I-V curves of individual cells of a module can be measured by completely shading the cell [1]. Differential I-V analysis and partial shading can be used to extract the shunt resistance and output current of individual cells in encapsulated modules [2]. Partial shading of cells in a module has also been used to extract their series resistance [3]. Shutter techniques have been used to access the response of individual cells in concentrating PV modules [4].

This work demonstrates a methodology for non-destructive automated current mapping of encapsulated PV modules without the need of cumbersome mechanical shading. Current mapping of PV modules is realised even in the presence of by-pass diodes without having to remove them or alter the structure of the PV module. The proposed approach utilises an alternative method for current mapping of PV devices based on the application of the compressed sensing (CS) sampling theory on LBIC measurements [5].

The CS sampling theory suggests that an N element signal can be measured by acquiring K observations, where K<<N [6][7]. With the standard LBIC method a point by point scan is performed by a light beam, reading the current response at every point to acquire the current map. When using CS current mapping a series of predefined random binary illumination patterns is projected on the sample. The current response is measured for each pattern and the final current map is acquired applying an optimisation algorithm. The main advantage of this technique is that fewer measurements are required to reconstruct the final current map than in standard LBIC measurements. This can lead to significantly shorter measurement times for current mapping. The signal to noise ratio is greatly increased, as almost half of the sample is illuminated by each pattern.

This technique has already been successfully applied to small area devices [8]. The initial small area experimental setup utilises a digital micromirror device chip (DMD) [9] in an optical system. In this work, a digital light processing (DLP) projector is utilised for CS current mapping of PV modules. DLP projectors are also based on a DMD chip, which actually creates the projection. Using a DLP based system for CS current mapping of PV modules shows some practical advantages when it comes to PV module current mapping. Such a system provides a perfect means to project the necessary partial shading and to project patterns on the sample under measurement for CS current mapping. Additionally, high signal to noise ratio for every projected pattern is achieved. Automated current mapping of cells in encapsulated modules is realised using this methodology. This is achieved by projecting patterns on the cell under measurement while light biasing the rest of the cells at the same time. This is the most significant advantage of this method, since any shading pattern can be implemented using a DLP projector. Current mapping of a PV module with by-pass diodes is achieved for the first time, without any mechanical shading.

2 COMPRESSED SENSING CURRENT MAPPING

In order to apply CS for acquiring measurements, a series of sampling functions $\{\varphi_m\}_{m=1}^{M}$ have to be projected on the PV device. Random binary matrices of ones and zeroes can be used as patterns, as they are easy to implement and satisfy the requirements for compressive sampling [10]. These matrices of ones and zeroes are translated to patterns of black and white pixels, to be projected on the sample. The patterns are expressed in a one row vector form, meaning that an $\sqrt{N}\cdot\sqrt{N}$ pixel square image is expressed as an N element vector. For every projected pattern, the current response of the PV device is

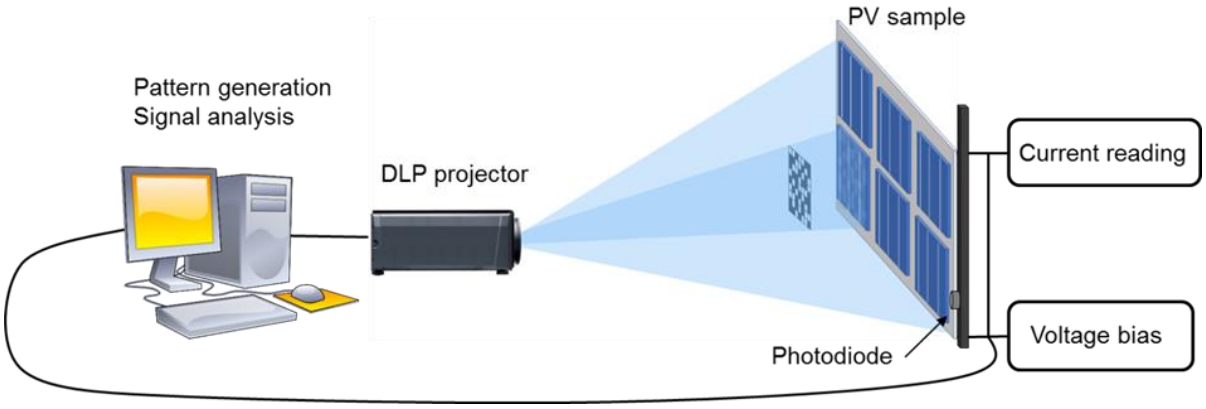

Figure 1: The experimental layout. An image is projected on the PV device. A part of it covering a single cell includes the specific pattern for compressive sampling while the rest of the cells are fully illuminated

measured, populating the measurement vector **y**. Since the projected patterns are known and included in the sensing matrix Φ, a solution to the underdetermined problem can be approximated by the **x** vector with the minimum ℓ1 norm [11], in other words:

$$\hat{\mathbf{x}}=\text{argmin}\|\mathbf{x}\|_1 \text{ subject to } \Phi\mathbf{x}=\mathbf{y}$$

With this method, current maps can be acquired with much fewer measurements than what a raster scan would require. This is because much fewer patterns than the pixels of the current map are projected on the sample. Using random patterns of 100 by 100 pixels, a 10000 pixel current map is acquired. The ℓ1 magic package in MatLab is used for reconstruction [12] and the primal dual ℓ1 minimisation algorithm is used from this toolbox. The time needed for reconstruction of the final current map is less than a minute, which is negligible compared to the data acquisition time. The CS current mapping procedure for PV devices is already analytically described in [8].

3 EXPERIMENTAL SETUP

The projector used for this work is a commercial Acer P7605 DLP projector with a 370W metal halide lamp. It is a reasonably high intensity projector, capable of generating a brightness of 5000 ANSI lumens. An important advantage of DLP technology is the high contrast ratio [13], which allows the system to efficiently generate a black pixel equivalent to a masked shaded spot on the PV module.

The basis of DLP projectors technology is the use of a beam of white light generated by the internal lamp. The beam is collimated and divided into its red, green and blue spectrum by a colour filter wheel. The micro-mirrors of the DMD operate at a frequency much higher than the human eye can perceive. The colour wheel is synchronised with the DMD and the colours are displayed at a very high rate so that eventually only the final combination of colours can be observed. This creates significant spectral and temporal variations of irradiance for PV characterisation. To overcome this limitation, the colour wheel of the projector was removed from the light path. In its final state, the projector only projects in black and white, the spectrum being the stable spectrum of the lamp.

Even without the colour wheel there are still periodic variations of intensity. The projector's internal DMD control behaves as if the colour wheel is still in place and is switching constantly, which leads to intensity variations. Although the projector's projections are controlled through LabVIEW environment, there is no absolute control of the internal DMD chip of the projector. The micromirrors that create the projections still turn on and off at a rate faster than 50 μs, causing temporal variations of irradiance on the sample's signal. These variations are short and periodic, with a period of approximately 4 ms. The signal of each period is averaged and recorded, and each current measurement averages 10 such readings, for reducing measurement noise due to intensity variation. Due to this reason, the sampling rate is very slow, approximately 2 samples per second.

The average absolute value of the irradiance on the sample plane is approximately 30W/m^2. This is significantly lower than what is used in standard test conditions for PV modules (1000W/m2), but it is adequate for acquiring valid measurement results in this study. The long term stability of the light source is also monitored simultaneously with the measurements, to ensure that any instability does not affect measurements. This is achieved using a photodiode installed next to the PV sample under test. A long term variation of light intensity of approximately 3.5% over a period of 30 minutes has been recorded.

This work uses 6-cell crystalline Silicon (c-Si) mini modules, which are produced in-house at CREST. All terminals of each individual cell were extended to the outside of the encapsulation, allowing direct contact with each cell

4 VOLTAGE BIAS CONSIDERATIONS FOR CURRENT MAPPING OF PV MODULES

When applying CS current mapping to a PV module, some implications of the applied voltage bias have to be considered. Ideally, when all the cells of the module are identical and uniformly illuminated, by setting the PV module to short circuit conditions (0V), each cell should individually be also at short circuit condition. With the projector as the light source, some small voltage differences for each cell arise due to the expected illumination non-uniformities. When CS sampling is applied, the patterns are projected onto one cell of the module while the rest are fully illuminated. If the PV module is biased to 0V, it is expected that the shaded cell

under measurement is actually reversed biased, while each of the others will be slightly forward biased, resulting in a sum of 0V for the module.

To verify this behaviour, all the cells of the custom mini-module are individually contacted and their voltage was measured while the PV module was biased at 0V. A sequence of 100 shading patterns are projected on one of the cells, each pattern increasing shading level (proportion of dark pixels randomly distributed over the area of the cell) by 1%. This means that the first projection fully illuminates all of the cells while the 100th projection fully shades one cell of the PV module while the other cells are fully illuminated. This test is applied to cell 1 and the results are presented in Figure 2. In the same figure, the voltage bias levels for all cells are indicated when all the cells are fully illuminated. This shows the effect of the non-uniformity of the projection. Nevertheless, as it will be demonstrated such non-uniformity issues do not prevent measurements to be applied.

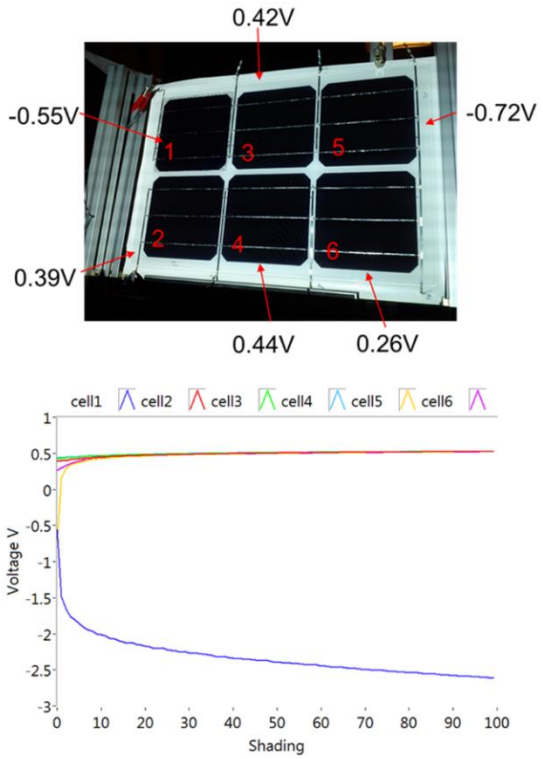

Figure 2: Top, the voltage bias of each cell when all the cells are fully illuminated and the module voltage is set to 0V. Bottom, the voltage levels of individual cells when cell1 is shaded with different shading levels

From Figure 2 it is clear that as shading is increased, the shaded cell becomes more reverse biased while the rest of the cells are forward biased as expected. This also shows that initial small non-uniformities of irradiance have no impact on voltage bias levels if one of the cells is shaded. In the case where one cell is underperforming compared to the others in the same module, it is reversed biased even when unshaded. To confirm this, similar defect-emulating masks to the previous section were used to reduce the output of some of the cells of the module. Three of the cells were covered with different sizes of these masks, as presented in Figure 3. The largest mask was placed on cell 3. When all the cells are illuminated, the cell with the largest mask is reversed biased, while all the others are forward biased at very similar levels. Running the same procedure as before and measuring the voltage of each cell while shading patterns are projected onto cell 5 (not masked), the graph at the bottom of Figure 3 is acquired.

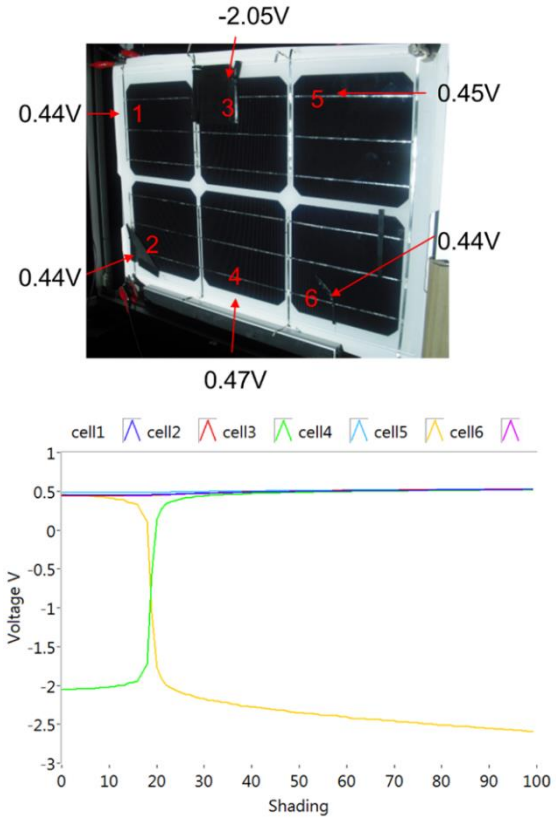

Figure 3: Top, voltage bias of each cell when all the cells are fully illuminated and the module voltage is set to 0V. Masks are applied on some of the cells. Bottom, the voltage levels of each cell when cell1 is shaded to different levels.

These results show that even if several cells of a module are underperforming, only the worst of them will be reversed biased. By increasing the shading levels on any of the rest of the cells, there is a point above which the shaded cell (and not the underperforming one) becomes reversed biased. The cell to be measured has to be the current limiting cell in a module, when applying CS current mapping. A forward voltage has to be applied to the module to bring the cell under test to operate close to short circuit conditions. Similar considerations and approaches have been applied for measuring spectral response of multijunction solar cells [14] and PV modules [15].

The same voltage measurements as above were applied with the the voltage bias set to 2.5V across the module terminals. This was not selected arbitrarily, but is just below the value of 5/6ths of the V_{OC} of the module (V_{OC}=3.15V) when all the cells are illuminated. Since for the patterns used for compressive sampling 40% of the pixels are at the "on" state (60% shading), the cell that is measured will be close to 0V when 2.5V forward bias is applied to the module.

This behaviour is confirmed in Figure 4 for cell1. By applying 2.5V forward bias to the module and for 60% shading, cell1 is close to short-circuit conditions (slightly forward biased ≃0.07V). When applying the patterns for

compressive sampling to the other cells, the forward voltage bias of the cell under test is in the region of 0.02V-0.08V for a module bias at 2.5V. Because in a PV module where individual cell contacts are inaccessible these direct measurements are not be possible, a module forward bias of $((N-1)/N)*V_{OC}$ should be applied as a rule of thumb. This ensures that the cell under measurement is always close to short-circuit conditions, or at least only very slightly forward biased. This voltage bias approach is not being introduced in this work, but has been reported and successfully applied in spectral response measurements [15] and angular response measurements of PV modules [16]. In our case, as long as any cell of the module does not perform less than 40% of the cell that is measured, CS current mapping measurements will be valid as the limiting cell will be that under measurement. More precisely, no cell should have similar performance with the measured (limiting) cell when the latter is illuminated with the patterns, as this will influence measurements. In that case, sparser sensing matrices (fewer pixels at the "on" state) can be used for meaningful measurements. This may decrease the SNR ratio of measurements but this approach is necessary for applying this method successfully.

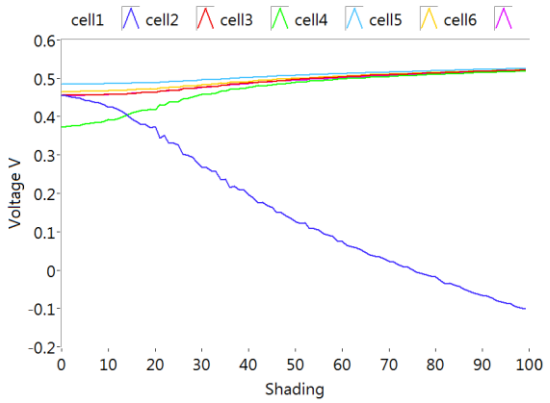

Figure 4: The voltage level of each cell of the custom module, when cell1 is shaded with different shading levels and the module is kept at 2.5V forward bias.

5 CURRENT MAPPING RESULTS FOR PV MODULES OF SERIES INTERCONNECTED CELLS

Following the individual cell test cases and the voltage bias considerations, the next step is to test whether CS current mapping of PV modules is practically feasible. Each cell is sampled with the necessary sensing patterns for compressive sampling consecutively, while the rest of the module is fully illuminated. All the cells are connected in series and the current is measured by contacting only at the PV module terminals.

As 100 by 100 pixel random patterns are used, the reconstructed current map of the entire PV module consists of 60000 pixels. Because of the slow sampling rate due to the previously described signal variations, measurement time was approximately 30 minutes for each cell. The reconstruction process is performed offline, using the $\ell 1$ reconstruction algorithm. This means that as soon as measurement acquisition of one cell has finished, the reconstruction process starts and the patterns move to the next cell at the same instant. The module voltage bias was set at 2.5V, as described in the previous section.

CS current mapping measurements with and without the defect-emulating masks are realised and presented in Figure 5. The current maps are acquired with 30000 measurements, an undersampling level of 50% of what a point by point scan would need. The measurement SNR value for these current measurements is approximately 1000. This is mainly due to the instability of the light source, as there is no direct control of the internal DMD of the projector.

These initial results using the custom mini module show that the projection approach for current mapping is a very convenient way for acquiring current maps of encapsulated PV modules. No mechanical shading is required to bring the cell under test to limiting conditions. The sampling patterns themselves not only realise the measurement but also provide the necessary shading that ensures the current limiting conditions.

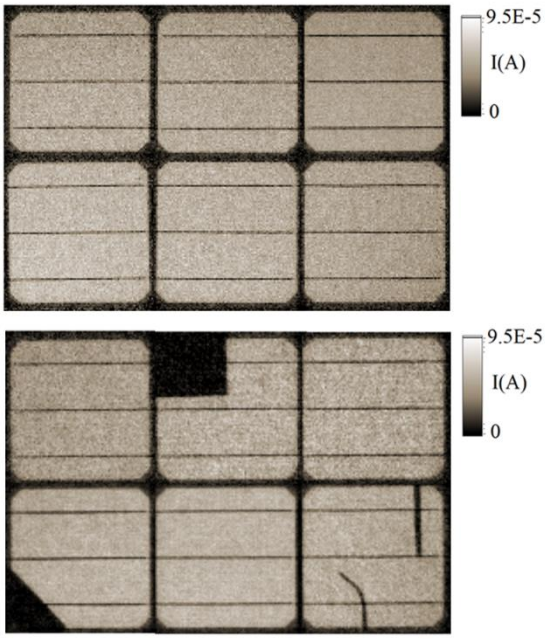

Figure 5: CS current map of the 6 cell PV module used in these experiments. The CS current map is produced having acquired 30000 (50%) measurements

The results show that the method works, even in the case with current mismatches between the cells. In reality, mismatches may exist in commercial PV modules, but such high levels of underperformance of individual cells are more likely to appear in aged or damaged PV modules rather than brand new ones. Some increased noise in the reconstructed maps is visible in the case of the masked cells and it affects the reconstruction process. This is more likely due to the current mismatch influencing measurements. Such issues were also observed in the case of LBIC measurements for PV modules with additional partial shading, where defects of individual cells were masked when contacting the module [17]. In the case of CS current mapping, this increases the noise levels of the reconstruction process.

6 BYPASS DIODES AND I-V CURVE CONSIDERATIONS

Commercial PV modules always have by-pass diodes

installed in order to avoid damage from reverse biased underperforming cells. However, this has implications when applying CS current mapping, since by-pass diodes provide alternate current paths for locally reverse biased cells or cell sub-strings. To establish what modifications to the CS method would be necessary in such a case, two by-pass diodes were added to the custom PV module used here. The PV module now consists of two sub-strings of three cells each with a bypass across. This was straightforward to implement since the contacts of each cell were already extended outside the module. The masks on three of the cells used in the previous section were also applied. The configuration of the PV module with the bypass diodes and defect-emulating masks is presented in Figure 6.

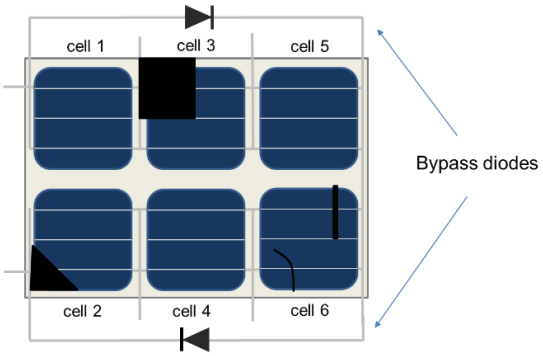

Figure 6: The configuration of the custom PV module of this work after installing two bypass diodes to create two sub-strings of three cells each

As a first step, the by-pass diodes were disconnected and a sequence of random patterns with increasing levels of shading is applied to one of the cells while the rest are fully illuminated, similarly with the voltage measurements of the previous section. I-V curves of the module for each shading level are acquired. This means that for the first I-V curve the cell is completely shaded (all pixels dark for this cell) while the last I-V curve is the same in all cases, as there is no shading at all. 10 of these I-V curves when each of cells 3 (large 'defect'), 4 (no defects) and 6 (two small 'defects') are shaded are presented in Figure 7.

.

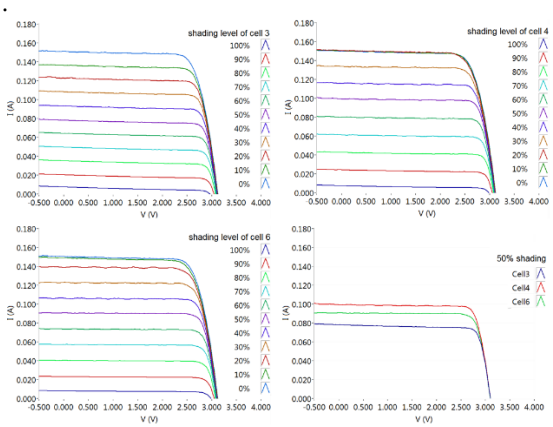

Figure 7: I-V curves of the PV module without by-pass diodes, acquired by shading one cell each time with different levels of shading. One I-V curve for each cell case with 50% shading is also included.

The I-V curves of the module for shading of any of the cells exhibit similar behaviour, while for 50% shading the maximum current depends on the performance of the cell shaded. This is precisely what makes CS current mapping work in the case that all the cells are connected in series. However, when by-pass diodes are installed, the I-V curves differ significantly from the case when all the cells are simply series connected. Following the same procedure as before to acquire the same series of I-V curves for shading the same three cells, the results of Figure 8 are acquired. It is noteworthy that even with no shading from the projector, the bypass diodes are activated at short circuit. This is due to the masks that have been applied on some of the cells, resulting in current mismatch that activates the by-pass diode of the worse string.

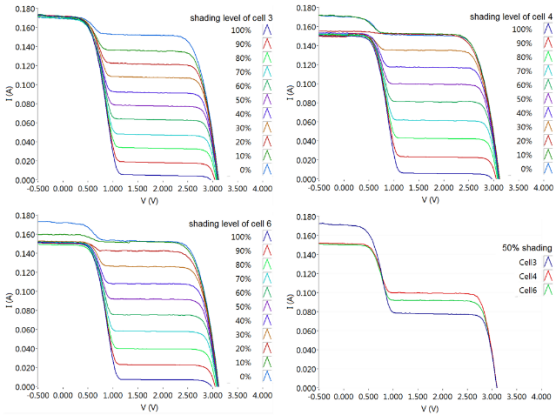

Figure 8: I-V curves of the PV module with bypass diodes, acquired by shading one cell each time with different levels of shading. One I-V curve for each cell case with 50% shading is also included.

For the application of CS current mapping measurements, a forward voltage bias as in the case of the previous section is necessary. Nevertheless, simultaneously with the voltage bias, an additional strategy is also adopted: by adjusting the projection on the PV module, one string is completely shaded, while the sub-string that includes the cell that is measured is properly illuminated. The patterns are projected on the cell under test and the rest of the cells of this specific sub-string are fully illuminated. The procedure is illustrated in Figure 9. As a first step, I-V curves are acquired as before, following this shading strategy. The results are presented in Figure 10. The influence of the shaded sub-string is almost negligible and it is barely visible at the bottom of the graphs, where a very low current exists for voltage values higher than 1.1V. If this voltage region is not considered, the I-V curves resemble those that would be acquired from a 3-cell mini module, with a small voltage drop. This is extremely convenient for the application of CS current mapping, since the current measured at the contacts of the PV module is only influenced by the limiting cell (measured cell) of the illuminated sub-string. This is clear when the I-V curves for 50% shading with this procedure for the three measured cells are displayed in the same graph. It is apparent that the current of the I-V in this instance depends on the performance of the cell of interest.

This above strategy where the sub-string not containing the cell under test is shaded is used for CS current mapping. A forward voltage bias of 0.6V is applied during measurements. This value was selected by considering the I-V curves of Figure 10. The illuminated cells of the module produce a voltage of around 1V, hence,

by choosing a forward bias of 0.6V the cell under test is operating very close to short-circuit conditions. This approach also shows that by acquiring the above I-V curves before measurements, one can reveal which cell underperforms. An initial diagnostic test can be set before CS current mapping measurements, where I-V curves are acquired with the same shading level for each cell while illuminating the rest of the string, following the above shading strategy for disabling cell sub-strings. Such tests are implemented in seconds. This procedure can reveal which cells underperform, the cells can be sorted depending on their performance and the correct forward voltage bias levels for the CS current mapping procedure can be chosen. More importantly, with this procedure the correct sparsity levels for the sensing matrices can be determined, to ensure that the patterns will shade the cells to a lower level than the output of the worst performing cell.

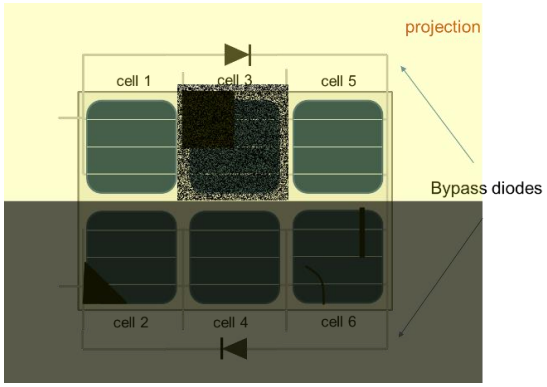

Figure 9: The process for CS current mapping measurements of a cell when by-pass diodes are installed in the module. The patterns are projected on the cell under test and the rest of the cells of this specific sub-string are fully illuminated, while the other sub-string is not illuminated.

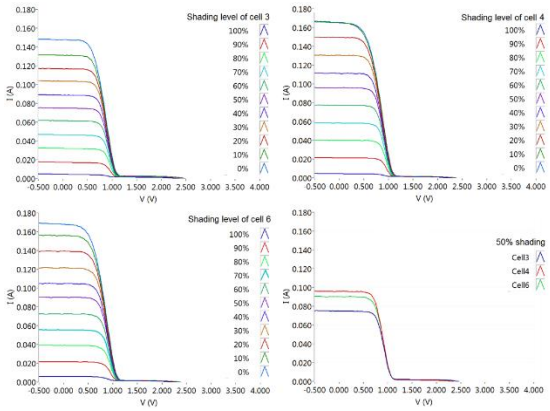

Figure 10: I-V curves of the PV module with by-pass diodes, acquired by shading one cell each time with different levels of shading, while completely shading the other string. One I-V curve for each cell case with 50% shading is also included.

Following the procedure of Figure 9 for all cells of the mini module with the by-pass diodes installed, the current map shown in Figure 11 is acquired. The reconstructed current map for an undersampling level of 50% (30000 measurements, 60000 pixels) is presented. In the same figure, a photograph of the module during measurements is also presented. The results are very similar to the case of the measurements for the mini module before installing by-pass diodes. The noise is slightly increased, since the average measurement SNR is reduced to ~700 after installing the bypass diodes. Nevertheless, meaningful measurements are acquired and this demonstrates for the first time that current mapping of a PV module with by-pass diodes can been achieved.

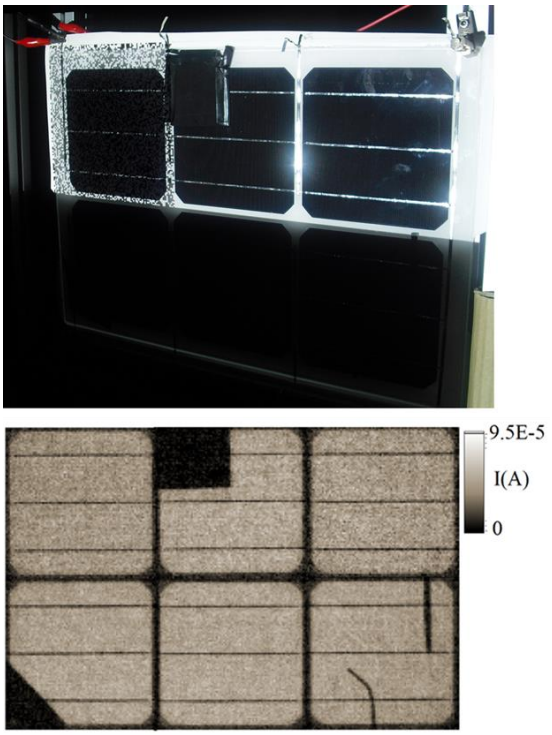

Figure 11: On top, a picture of the PV module during measurement when bypass diodes are included. Bottom, the CS current map of the PV module with by-pass diodes at 50% undersampling.

7 CONCLUSIONS

Non-destructive, automated current mapping of PV modules has been demonstrated in this work. Current maps of individual PV cells in encapsulated modules can be acquired without having to tap the cells, remove bias diodes or use mechanical shading. The approach includes a prototype DLP projection based current mapping system that has been developed at CREST, which utilizes a commercial DLP projector and compressive sampling for current mapping of PV devices.

The demonstrated methodology can become a very useful tool for spatial characterisation of crystalline silicon based or thin film PV modules. The tools utilised to achieve this approach exhibit some very practical properties for spatial characterisation. CS current mapping always requires fewer measurements than what a raster scan would need. The measured signal is significantly amplified due to the projection of patterns instead of a raster scan, resulting in an enhanced measurement SNR.

Experimental results prove that a custom DLP projector based CS current mapping system for PV modules is feasible. DLP projection technology is a perfect means for creating and projecting structured illumination

patterns for current mapping of PV modules. Specific shading strategies were developed in order to isolate the cell under test. It is demonstrated that such shading strategies can also be applied to acquire I-V curves of the module to detect if any of its cells is underperforming. This diagnosis process takes seconds using the DLP projector and can sort the cells of a module in order of performance, even in the presence of by-pass diodes. This can also be useful in order to determine the sensing matrix sparsity necessary for CS current mapping measurements.

As discussed already, this prototype system cannot achieve very high accuracy and optical resolution as it uses a commercial DLP projector. This is mainly because of the high noise levels and the low irradiance produced by this system. A custom system will provide more control on the DMD chip and will be able to reduce temporal variations of light intensity. This would decrease noise levels and provide higher accuracy. Latest advances in high power DLP display technology for cinema applications can be utilized for increasing optical power. The proposed measurement method and system aids to the development of a realistic solution for current mapping of PV modules. Moreover, the approaches and strategies demonstrated can also be utilised to develop additional characterisation tools for PV modules based on DLP technology and the CS theory.

ACKNOWLEDGMENTS

This work was funded through the European Metrology Research Programme (EMRP) Project 16ENG02 PV-Enerate. The EMRP is jointly funded by the EMRP participating countries within EURAMET and the European Union. This work is co-funded by the UK National Measurement System.

REFERENCES

[1] L. De Bernardez and R. H. Buitrago, “Dark I–V curve measurement of single cells in a photovoltaic module,” *Prog. Photovoltaics Res. Appl.*, vol. 14, no. 4, pp. 321–327, 2006.

[2] G. B. B. Alers, J. Zhou, C. Deline, P. Hacke, and S. R. R. Kurtz, “Degradation of individual cells in a module measured with differential IV analysis,” *Prog. Photovoltaics Res. Appl.*, vol. 19, no. 8, pp. 977–982, 2011.

[3] Y. S. Kim, S. M. Kang, B. Johnston, and R. Winston, “A novel method to extract the series resistances of individual cells in a photovoltaic module,” *Sol. Energy Mater. Sol. Cells*, vol. 115, pp. 21–28, 2013.

[4] M. D. Yandt, J. P. D. Cook, K. Hinzer, and H. Schriemer, “Shutter technique for noninvasive individual cell characterization in sealed CPV modules,” *IEEE J. Photovoltaics*, vol. 5, no. 2, pp. 691–696, 2015.

[5] S. R. G. Hall, M. Cashmore, J. Blackburn, G. Koutsourakis, and R. Gottschalg, “Compressive Current Response Mapping of Photovoltaic Devices Using MEMS Mirror Arrays,” *IEEE Trans. Instrum. Meas.*, vol. 65, no. 8, pp. 1945–1950, 2016.

[6] D. Donoho, “Compressed sensing,” *IEEE Trans. Inf. Theory*, vol. 52, no. 4, pp. 1289–1306, Apr. 2006.

[7] E. J. Candès, J. K. Romberg, and T. Tao, “Stable signal recovery from incomplete and inaccurate measurements,” *Commun. Pure Appl. Math.*, vol. 59, no. 8, pp. 1207–1223, 2006.

[8] G. Koutsourakis, M. Cashmore, S. R. G. Hall, M. Bliss, T. R. Betts, and R. Gottschalg, “Compressed Sensing Current Mapping Spatial Characterization of Photovoltaic Devices,” *IEEE J. Photovoltaics*, vol. 7, no. 2, pp. 486–492, Mar. 2017.

[9] L. J. Hornbeck, “The DMDTM Projection Display Chip: A MEMS-Based Technology,” *MRS Bull.*, vol. 26, no. 04, pp. 325–327, Apr. 2001.

[10]R. Baraniuk, M. Davenport, R. DeVore, and M. Wakin, “A Simple Proof of the Restricted Isometry Property for Random Matrices,” *Constr. Approx.*, vol. 28, no. 3, pp. 253–263, Jan. 2008.

[11]R. G. Baraniuk, “Compressive Sensing,” *IEEE Signal Process. Mag.*, vol. 24, no. July, pp. 118–121, 2007.

[12]E. J. Candes, J. Romberg, and T. Tao, “Robust uncertainty principles: exact signal reconstruction from highly incomplete frequency information,” *IEEE Trans. Inf. Theory*, vol. 52, no. 2, pp. 489–509, Feb. 2006.

[13]D. S. Dewald, D. J. Segler, and S. M. Penn, “Advances in contrast enhancement for DLP projection displays,” *J. Soc. Inf. Disp.*, vol. 11, no. 1, p. 177, 2003.

[14]J. Burdick and T. Glatfelter, “Spectral response and I-V measurements of tandem amorphous-silicon alloy solar cells,” *Sol. Cells*, vol. 18, no. 3–4, pp. 301–314, 1986.

[15]Y. Hishikawa, Y. Tsuno, and K. Kurokawa, “Spectral Response Measurements of PV Modlues and Multi-Junction Devices,” in *22nd European Photovoltaic Solar Energy Conference (22nd EU PVSEC)*, 2007, pp. 2765–2769.

[16] W. Herrmann, M. Schweiger, and L. Rimmelspacher, “Solar Simulator Measurement Procedures for Determination of the Angular Characteristic of PV Modules,” in *29th European Photovoltaic Solar Energy Conference (29th EU PVSEC)*, 2014, vol. 2, pp. 2403–2406.

[17]P. Vorasayan, T. R. Betts, and R. Gottschalg, “Limited laser beam induced current measurements: a tool for analysing integrated photovoltaic modules,” *Meas. Sci. Technol.*, vol. 22, no. 8, p. 085702, Aug. 2011.